Thermal decomposition kinetics of functionalized polynorbornene

Michael D. Wedlake and Paul A. Kohl[a)]
School of Chemical Engineering, Georgia Institute of Technology, Atlanta, Georgia 30332-0100

(Received 1 June 2001; accepted 2 January 2002)

The mechanism and kinetic parameters for the thermal decomposition of four functionalized addition-polymerized polynorbornenes were studied by dynamic and isothermal thermogravimetric analyses and by mass spectrometry. The dynamic and isothermal thermogravimetric analyses showed a first-order degradation reaction mechanism with an activation energy of 229.6 ± 12.5 kJ/mol. Based on the polymer structure, reference mass spectra for related molecules, and a cross-comparison of the mass spectra, the backbone, free-radical scission mechanism was found to occur by cleavage of the linkages between bicyclic rings and the production of volatile monomer and oligomers. The degradation of polynorbornene occurred via a depropagation and transfer reaction process. Initially, the depropagation pathway was preferred, but with increasing conversion, intra- and intermolecular hydrogen transfer reactions dominated.

I. INTRODUCTION

The synthesis of polynorbornene or poly(bicyclo[2.2.1]-hepte-2-ene) (PNB) was first described by Anderson *et al.*[1] Two types of polymers were formed: a brittle, saturated, low molecular weight, addition polymer and a ring opening metathesis polymerization (ROMP) material. The former material possesses a saturated backbone consisting of linked, fully intact norbornane-type molecules. It has excellent thermal stability. The synthesis method was later refined by McKeon using reaction conditions that would enable the selective production of either the ROMP or addition polymerization.[2] Kaminsky reported that addition-polymerized PNB can be produced in the amorphous and highly crystalline forms.[3,4] Due to low solubility and lack of a suitable melting point, the crystalline material is difficult to process, and the focus shifted to the amorphous material. A facile addition polymerization route using an organo (nickel or palladium) complex was found for synthesizing amorphous PNB.[5] There are numerous publications on the subject.[6–13]

The addition-polymerization route allows considerable freedom to tailor the two critical aspects: tight control of the molecular weight and flexibility in choice of side-groups on the norbornene repeat unit. This has allowed synthesis of a wide variety of functionalized polynorbornenes with a variety of mechanical, thermal, and electrical properties. Several functionalized polynorbornenes have been described by Grove.[14] Some of the attributes that make PNB attractive include excellent thermalperformance (glass transition temperature T_g exceeding 350 °C), excellent adhesion to a wide variety of materials, low moisture absorption (<0.1%), and low dielectric constant (2.2–2.6).[14] In addition to the use of polynorbornene as a low dielectric constant insulator,[14] it is also being investigated as an optical material,[15] a backbone for 157 nm photoresist,[16] and a gas membrane.[17]

Another use for polynorbornene is as a sacrificial material. At temperatures above its degradation temperature, PNB will break down into a volatile species. When encapsulated within an appropriately porous material such as plasma-enhanced chemical vapor deposited silicon oxide and nitride or polyimide, these gases can diffuse out leaving behind hollow cavities that can be formed in regions previously occupied by the polymer.[18] Understanding and controlling the thermal degradation of PNB is thus a critical component of this process. In the work reported in this paper, the mechanisms and kinetics of the thermal degradation of several functionalized polynorbornenes were studied using thermal gravimetric analysis and mass spectrometry.

II. EXPERIMENTAL

Three different alkyl polynorbornenes were analyzed: methyl-, butyl-, and hexyl-PNB (MePNB, BuPNB, and HxPNB, respectively). In addition, a copolymer of 90 mol% butyl PNB and 10 mol% triethoxysilyl (TES) PNB (BuTESPNB) was studied. All polymers were kindly donated by the BF Goodrich Corporation (Brecksville, OH). The average molecular weights for these polymers were found to be: 198,000 (MePNB), 185,000 (BuPNB), 195,000 (HxPNB), and 300,000 (BuTESPNB), as determined by the manufacturer.

[a)]Address all correspondence to this author.
e-mail: paul.kohl@che.gatech.edu

Dynamic and isothermal thermal gravimetric analysis (TGA) experiments were performed on 10 to 20 mg samples using a Seiko Instruments Inc. 320 thermogravimetric differential thermal analyzer (Haake Instruments, Paramus, NJ). The degradation chamber was purged with high purity nitrogen (99.998%, excluding Argon) prior to analysis so that the residual oxygen concentration was less than 50 ppm as measured by an Alpha Omega Instruments Series (Stanford, CT) 3000 trace oxygen analyzer. The sample chamber was continuously purged with nitrogen during the experiments. The samples were first heated to 290 °C and held for 10 mins to remove any residual solvent or volatile, low molecular weight impurities. This was followed by heating the sample at a specific constant ramp rate in the dynamic TGA experiments. The isothermal experiments involved rapid heating (100 °C/min) of the sample to the desired temperature, followed by a temperature hold until degradation was complete. The dynamic experiments involved ramping the sample at a constant heating rate until the polymer had volatilized.

The mass spectrometer used was a Vacuum Generators 70SE (Est Sussex, UK) double focusing high resolution mass spectrometer interfaced to an 11-250 data acquisition and processing system. The standard electron energy of 70 eV was used for these experiments. The samples were packed into 2-mm outer diameter quartz capillaries and degraded inside the mass spectrometer. The volatile species exiting the capillary were introduced directly to the ionization chamber at high pressure of 10^{-5} to 10^{-6} torr. The mass spectrometer was equipped with a heated stage and scanned from 35 to 800 amu.

III. RESULTS AND DISCUSSION

The dynamic TGA results for BuTESPNB are shown in Fig. 1. The weight percentage remaining after degradation is plotted versus temperature. All of the curves show the same sigmoidal shape independent of the temperature ramp rate. The isothermal TGA traces for the same polymer, BuTESPNB, are plotted in Fig. 2 as a weight percentage remaining versus time. Like the dynamic TGA traces, the isothermal curves show a single weight drop. The degradation rate is seen to increase with increasing temperature (steeper slope). Based on the shapes of the TGA data, a simple degradation model was proposed:

$$-\frac{dW}{dt} = A \exp\left(\frac{-E_a}{RT}\right) W^n \quad , \tag{1}$$

where W is the weight (excluding final residue), t is the time, $-dW/dt$ is the experimentally measured weight loss rate, A is the pre-exponential constant, E_a is the

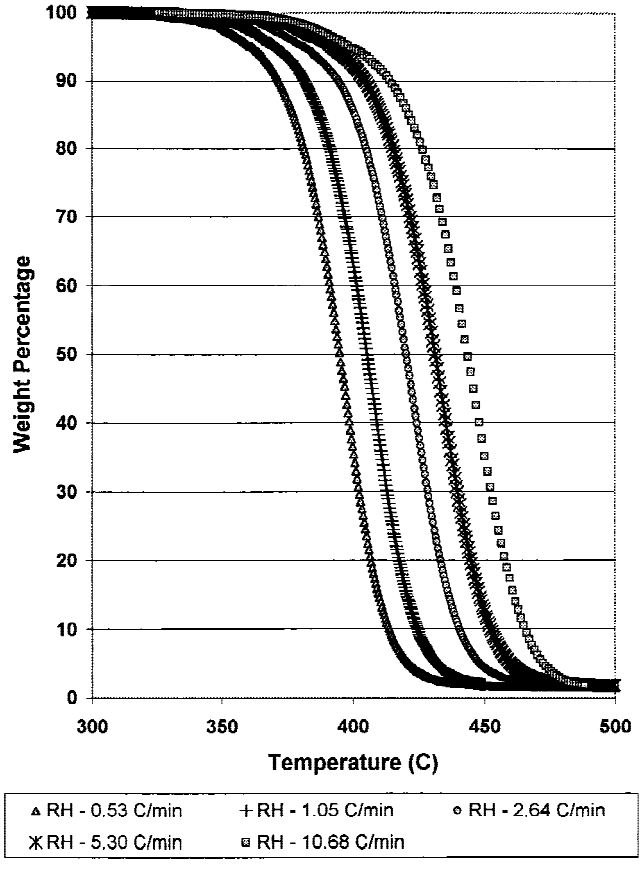

FIG. 1. Weight percentage versus temperature for dynamic TGA of BuTESPNB for various rates of heating.

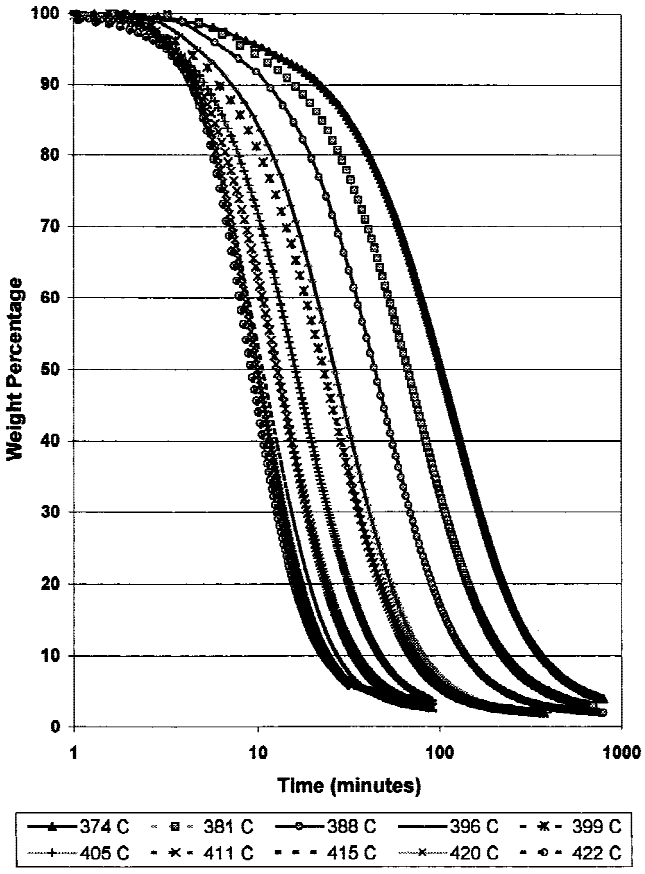

FIG. 2. Weight percentage versus time for isothermal BuTESPNB TGA.

activation energy, R is the ideal gas constant, T is the absolute temperature, and n is the reaction order. In the case of a constant rate of heating (RH) (as in the dynamic TGA experiment), Eq. (1) can be transformed to Eq. (2):

$$-\frac{dW}{dT} = \frac{A}{RH}\exp\left(\frac{-E_a}{RT}\right)W^n \quad . \tag{2}$$

Materials that behave according to these models may be analyzed by the Ozawa method.[19] Using the integral approximation suggested by Reich,[20] the activation energies were individually calculated at every 5% conversion between 10% and 90% conversion using the following relationship:

$$\log\left(\frac{RH}{T^2}\right) = \left(\frac{-E_a}{2.3\ RT}\right) + \text{const} \quad . \tag{3}$$

A plot of the left side of Eq. (3) versus inverse absolute temperature at a particular value of conversion yields a straight line, the slope of which gives the activation energy. The data from Fig. 1 was replotted according to Eq. (3) and is shown in Fig. 3 for BuTESPNB. The data in Fig. 3 showed an excellent linear fit ($R^2 > 0.999$). The average activation energy for BuTESPNB was 236.8 kJ/mol with a standard deviation of 4.7 kJ/mol. Once the activation energy was determined, the two other kinetic parameters could be determined by manipulating Eq. (2) to give Eq. (4):

$$\ln\frac{-\frac{dW}{dT}}{\exp\left(\frac{-E_a}{RT}\right)} = n\ \ln\ W + \ln A \quad . \tag{4}$$

A plot of the left side of Eq. (4) versus the natural logarithm of weight will yield a straight line with a slope equal to the reaction order and a y intercept directly related to the pre-exponential constant. Figure 4 shows examples of the result for BuTESPNB. The slope and y

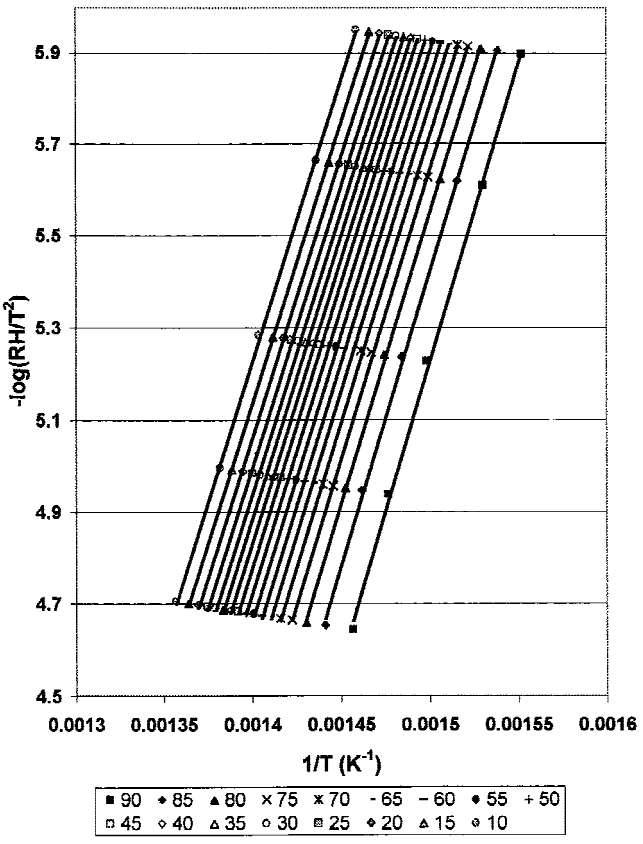

FIG. 3. Negative logarithm of heat rate divided by absolute temperature squared versus inverse absolute temperature for BuTESPNB at various conversion percentages.

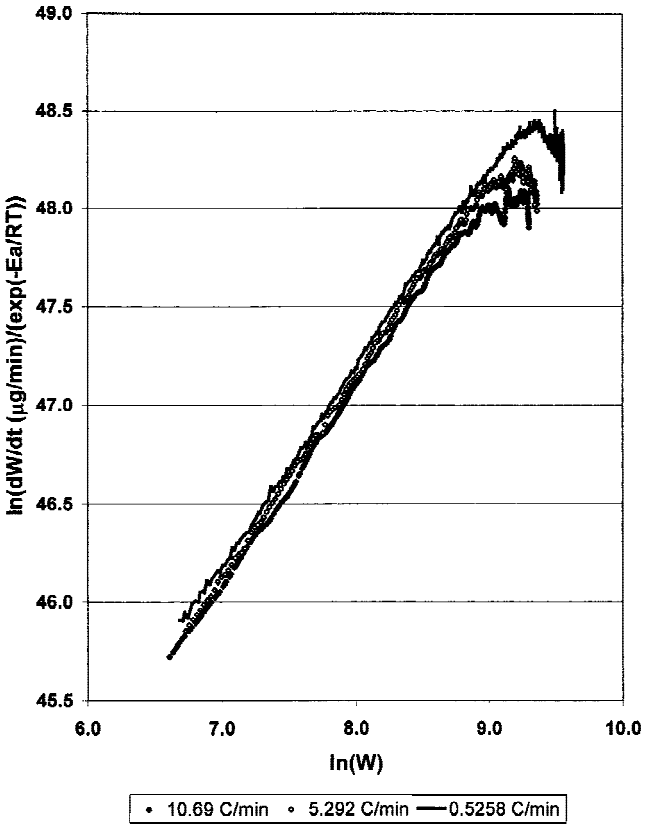

FIG. 4. Natural logarithm of weight loss rate (mg/min) divided by the Arrhenius exponential term using E_a = 236.7 kJ/mol versus the natural logarithm of corrected weight (mg) for dynamic BuTESPNB TGA.

intercept from the linear region of Fig. 4 (from 40% conversion to 90% conversion) were used to calculate the kinetic parameters. This corresponds to the bulk of the degradation process. A small degree of variation in the degradation rate during the initial conversion produced a nonlinear region between 0% and 40% conversion in Fig. 4. This deviation is accentuated by the logarithmic nature of Eq. (4).

The origin of this deviation could have many sources. One drawback of using thermogravimetric techniques to determine polymer degradation kinetics is an inability to describe structural changes occurring in the polymer other than those that produce volatile species. During the initial stages of degradation, the vibrational energy released through the cleavage of weak links in the polymer chain produce smaller chain segments. Some of these preliminary steps will not produce volatile products and are therefore hidden from the kinetic model developed from the TGA data. In general, the volatilization rate was consistently lower during the early stages of degradation than predicted by the first-order model. With increasing conversion, the margin between the experimental data volatilization rate and the simple first-order model shrank. The data collected from the initial 40% conversion was excluded from the analyses because thermogravimetric analysis cannot account for polymer degradation that does not involve the release of volatile species. The reaction order was found to be 0.99 ± 0.01 and the pre-exponential constant was measured to be $1.09 \times 10^{17} \pm 0.05 \times 10^{17}$ min^{-1}.

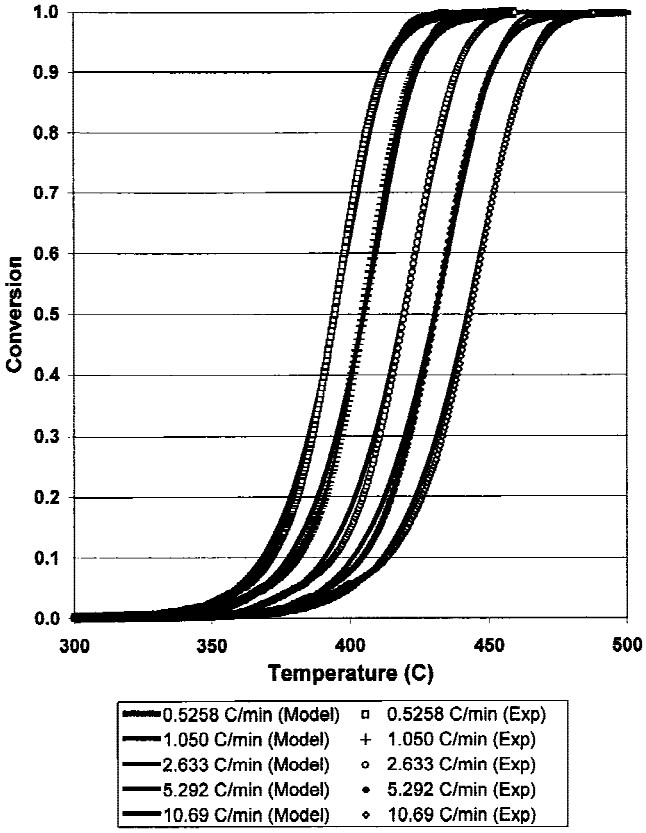

FIG. 5. Conversion versus temperature comparison for the first-order kinetic model with activation energy of 232.1 kJ/mol and pre-exponential constant of 6.66×10^{16} min^{-1} and the experimental data.

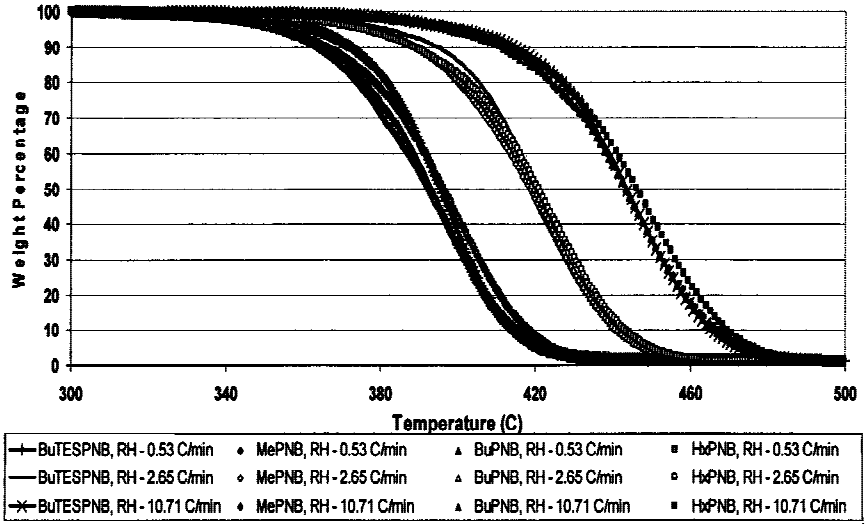

FIG. 6. Comparison of BuTESPNB, MePNB, BuPNB, and HxPNB dynamic TGA traces at RH of 0.53 ± 0.01 °C/min (grey shapes, left), 2.65 ± 0.02 °C/min (white shapes, center), and 10.75 ± 0.06 °C/min (black shapes, right).

To validate these measurements, the isothermal TGA data was analyzed. Under isothermal conditions, the reaction rate k will remain constant:

$$k = \mathrm{A}\exp\left(\frac{-E_\mathrm{a}}{\mathrm{R}T}\right) \quad . \tag{5}$$

Substituting Eq. (5) into Eq. (1) and manipulating gives Eq. (6):

$$\ln\left(-\frac{\mathrm{d}W}{\mathrm{d}t}\right) = n\ln W + \ln k \quad . \tag{6}$$

A plot of $\ln(-\mathrm{d}W/\mathrm{d}t)$ versus $\ln W$ yields a straight line with a slope equal to the reaction order and a y intercept related to the reaction rate. Manipulating Eq. (5) yields:

$$\ln k = \frac{-E_\mathrm{a}}{\mathrm{R}T} + \ln \mathrm{A} \quad . \tag{7}$$

A plot of $\ln(k)$ versus inverse temperature yields a plot whose slope is related to the activation energy and whose y intercept is related to the pre-exponential constant. After 40 wt% conversion, these values were measured for the isothermally degraded BuTESPNB. At low values of weight loss, the isothermal temperature was not yet reached. The kinetic parameters were found to be $n = 1.04 \pm 0.07$, $E_\mathrm{a} = 228.0 \pm 6.7$ kJ/mol, and $\mathrm{A} = 2.24 \times 10^{16} \pm 0.06 \times 10^{16}\ \mathrm{min}^{-1}$.

The kinetic parameters obtained from the dynamic and isothermal TGA agree reasonably well. Both indicate first-order kinetics, and their activation energy ranges overlap within the uncertainty of the experiments. Figure 5 shows a plot of the conversion versus temperature using $n = 1.00$, $E_\mathrm{a} = 232.1$ kJ/mol, and $\mathrm{A} = 6.66 \times 10^{16}\ \mathrm{min}^{-1}$. The model shows a good fit with the experimental data although there is systematic overprediction of the degradation rate at low

TABLE I. Kinetic Parameters for the AlkylPNBs.

	MePNB	BuPNB	HxPNB
Avg. E_a (kJ/mol)	223.1	228.3	229.9
St. Dev. E_a (kJ/mol)	6.3	4.2	4.8
Avg. n (kJ/mol)	1.02	1.01	1.00
St. Dev. E (kJ/mol)	0.02	0.03	0.05
Avg. A (min^{-1})	8.69×10^{16}	2.10×10^{16}	2.30×10^{16}
St. Dev. A. (min^{-1})	0.46×10^{16}	0.07×10^{16}	0.11×10^{16}

Avg.: average; St. Dev.: standard deviation.

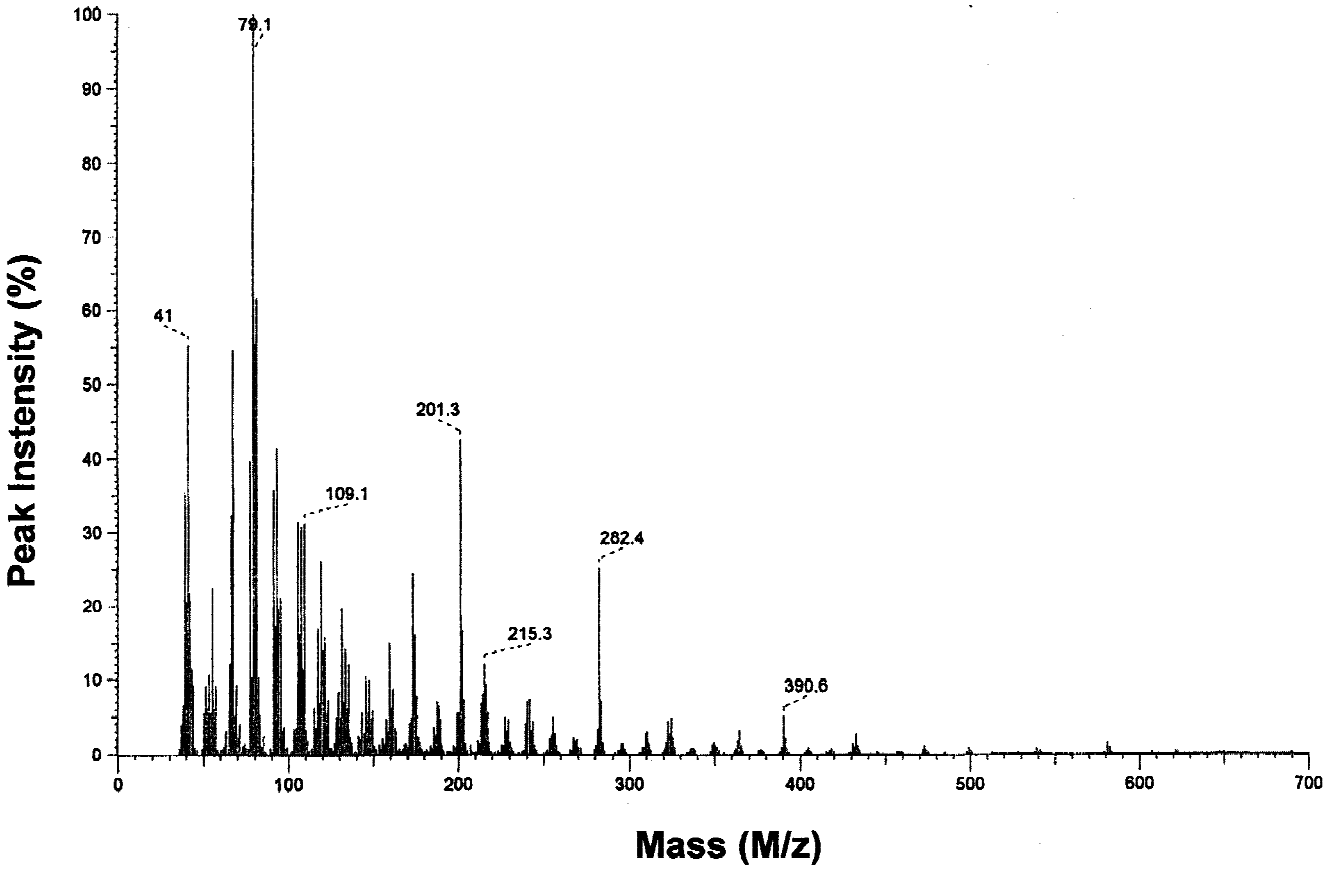

FIG. 7. Mass spectrum of methyl polynorbornene at 400 °C.

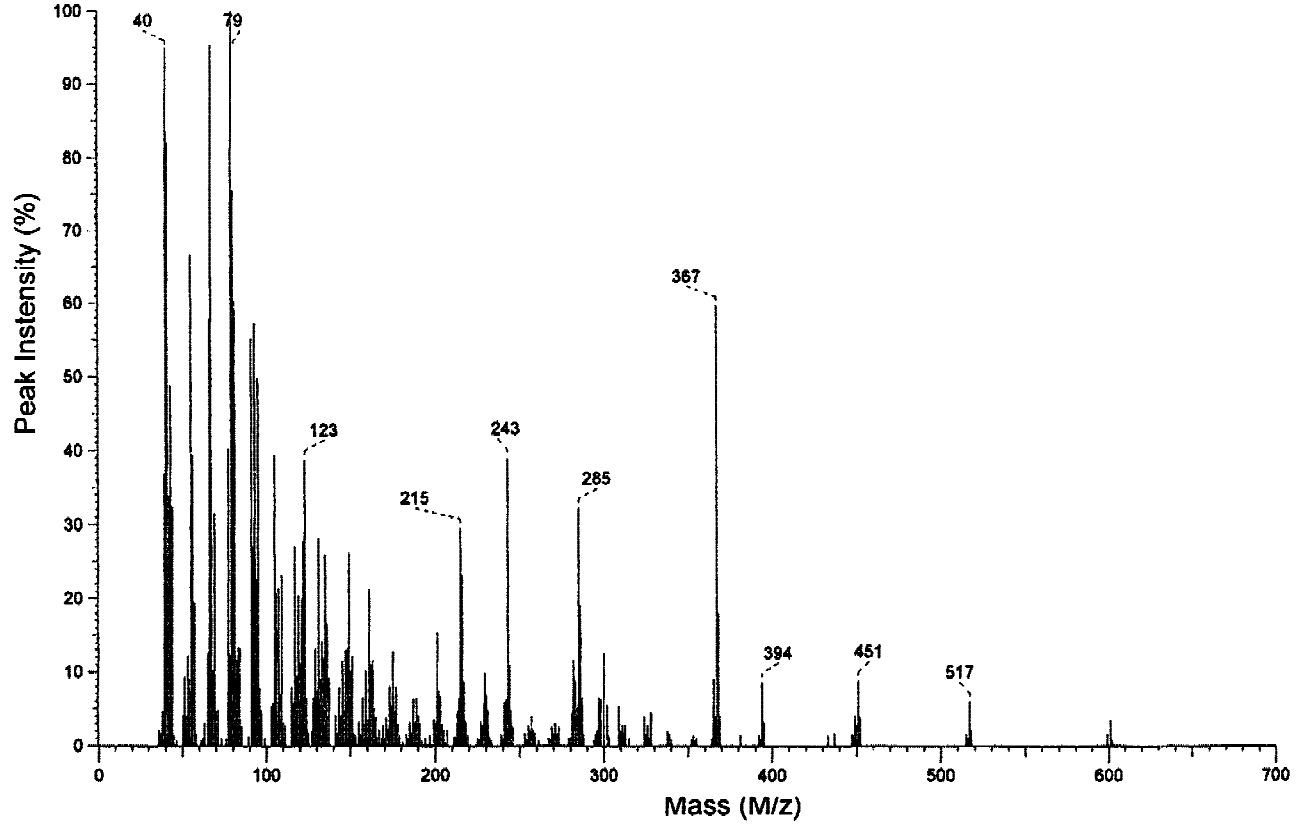

FIG. 8. Mass spectrum of butyl polynorbornene at 400 °C.

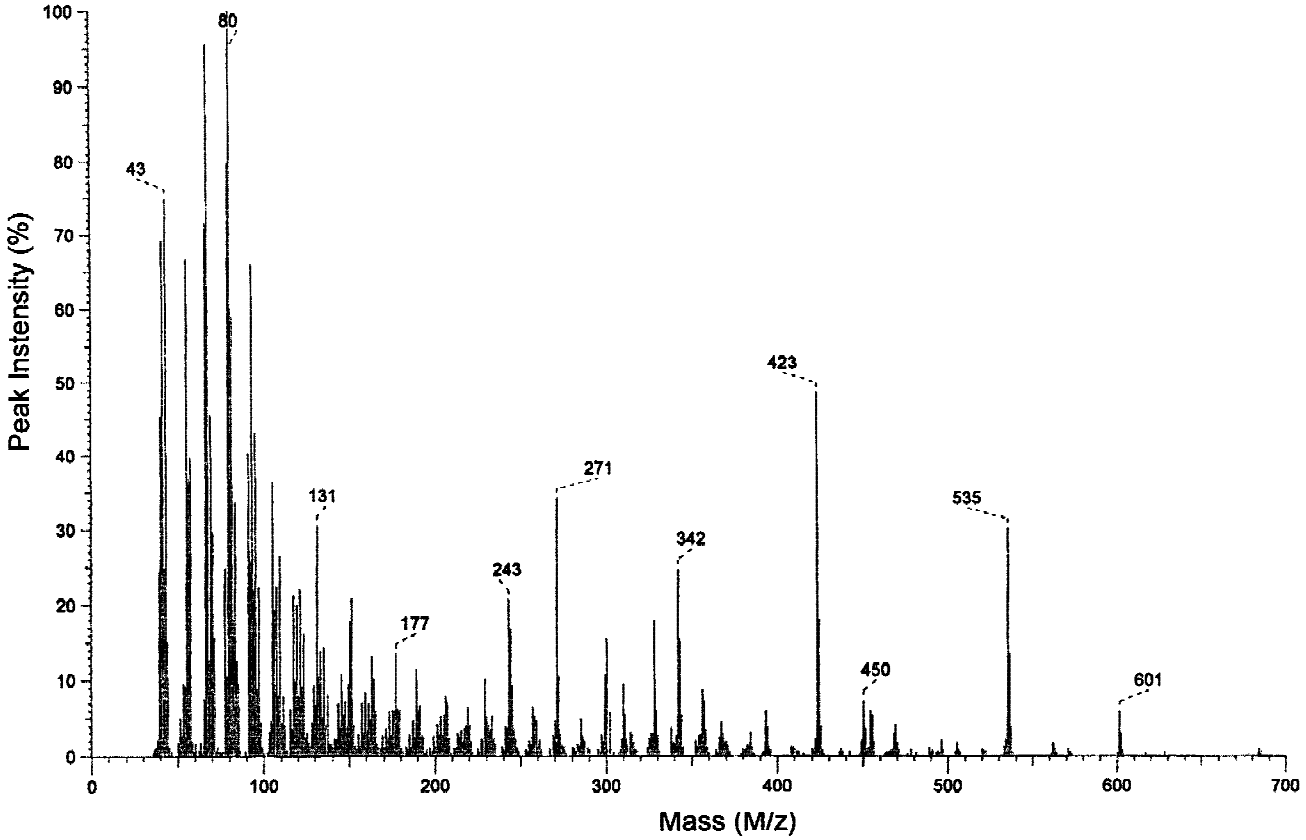

FIG. 9. Mass spectrum of hexyl polynorbornene at 400 °C.

conversions. This deviation can be best understood after describing the results of the three other alkylPNBs and the mass spectrometry results and discussion.

MePNB, BuPNB, and HxPNB were analyzed in a similar manner to BuTESPNB. Due to limited quantities of each material, only three dynamic and three isothermal experiments were performed. Figure 6 shows the dynamic TGA for these materials as well as BuTESPNB at ramp rates of 0.53 ± 0.01, 2.65 ± 0.02, and 10.75 ± 0.06 °C/min. This plot shows that all four of the polymers exhibited a similar degradation behavior and that the pendant side groups had little effect on the temperature or rate of degradation. The most important exception is the deviation of the BuTESPNB between 0% and 35% conversion. It appears that the inclusion of the triethoxysilane group may have an initial stabilizing effect on the cyclic rings, possibly as a result of the changing electron valencies for this heteroatom containing side group.[20] The order of the polymers in terms of increasing thermal stability is MePNB, BuPNB, HxPNB, and BuTESPNB. The kinetic parameters calculated using the dynamic TGA can be found in Table I.

The degradation mechanism of polynorbornene is consistent with the degradation of other linear polyolefins. The bulk degradation mechanism is influenced by the ratio of depropagation to transfer which is dependent on the reactivity of the free radicals produced in the initiation process and on the availability of reactive atoms in the polymer systems (namely hydrogen). Depropagation reactions produce high yields of monomer while transfer reactions produce oligomers. Because transfer reactions tend to cause fragmentation of the polymer chains, a large drop in the molecular weight occurs before appreciable volatilization. This is consistent with the degradation kinetics described for polynorbornene.

The compositions of the gases produced from thermal degradation of PNB were investigated by mass spectrometry. The mass spectra for the decomposition of MePNB, BuPNB, HxPNB, and BuTESPNB can be found in Figs. 7, 8, 9, and 10, respectively. These spectra show the major mass-to-charge peaks up to 800 amu observed during degradation under vacuum. The first task was to assign hydrocarbon identities to the major peaks. Since the product species identified in the mass spectra are the primary fragments produced during the ionization step in the mass spectrometer, the original pyrolysis product gases can be determined only by piecing together the fragmented parts. To understand the mechanism of degradation, reference mass spectra were consulted. The most important of these were the mass spectra for

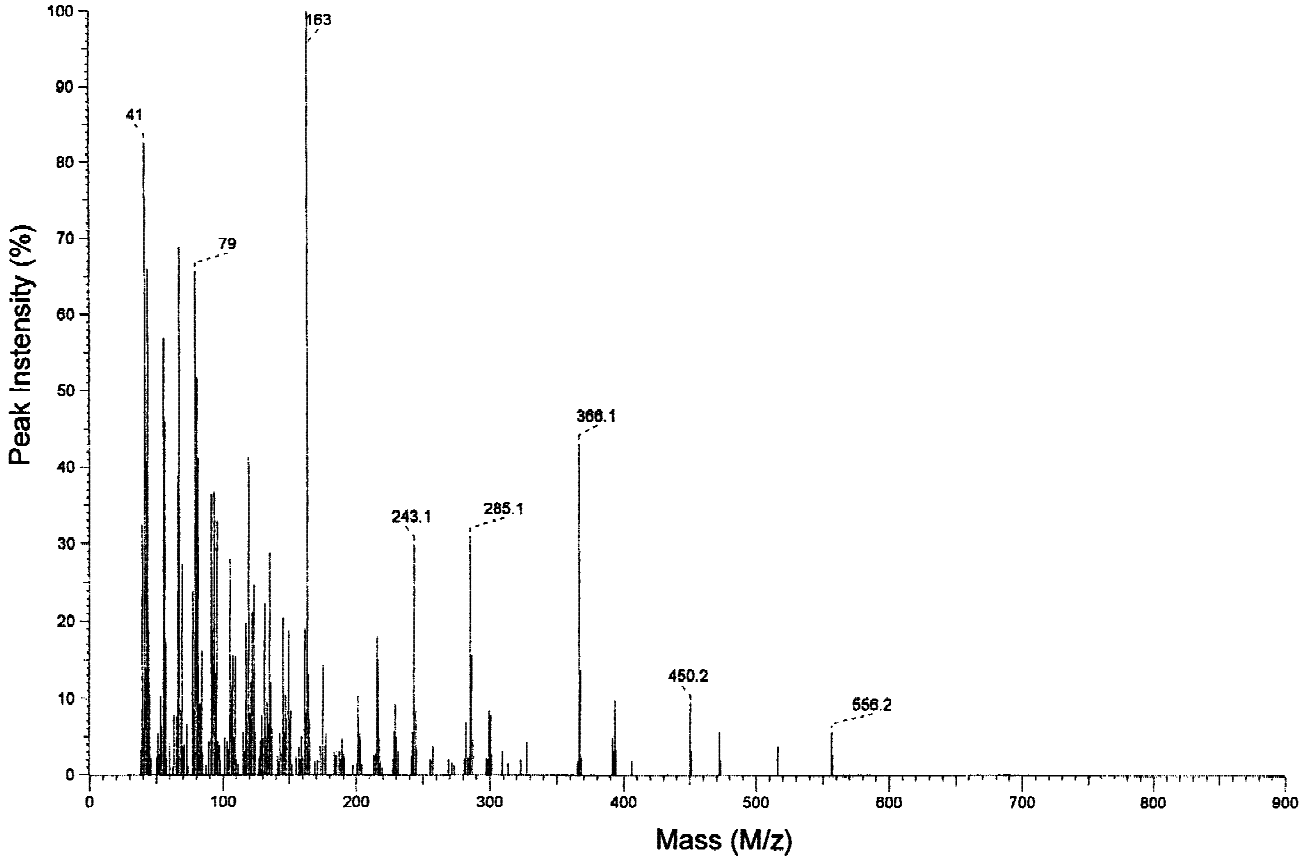

FIG. 10. Mass spectrum of butyl (90 mol%) triethoxy silyl (10 mol%) polynorbornene at 400 °C.

the related compounds norbornane and norbornene. Based on the degradation mechanism, Fig. 11 shows the proposed methods of backbone scission.[22,23] In the transfer reaction, a double bond is formed in the chain. However, since the fragment may be composed of more than one monomer repeat unit, the double bond will only be found at one end. The remainder of the fragment will be composed of linked saturated oligomers. If polynorbornene degraded exclusively by depropagation (i.e., the loss of single repeat units), the components one would find in the mass spectrum would be identical to those in the norbornene spectrum, namely 66.

The four derivatives of polynorbornene (different side groups) investigated in this study provided a valuable tool for peak identification. That is, the molecular weight of the methyl, butyl, and hexyl PNB are separated only by the difference in the alkyl side groups. Bu/TESPNB is a random copolymer and would have the same peaks as BuPNB in addition to other due to TESPNB. Figure 12 shows the most probable peak identifications for the four polymers used in this study. The peaks found in Figs. 7–10 show a consistent set of peaks distinguished by their side groups. The inclusion of the TESPNB unit (10 mol%) with BuPNB (90 mol%) can be seen in Fig. 10, versus Fig. 8 for pure BuPNB. The triethoxysilane side group contributed the peaks at 163, 472, and 556. Mass 163 corresponds to the fragmented TES group, and the higher molecular weight species are shown in Fig. 13.

The polynorbornenes were studied using time resolved mass spectra under isothermal and dynamic (ramped temperature) conditions. In each case, the majority of the

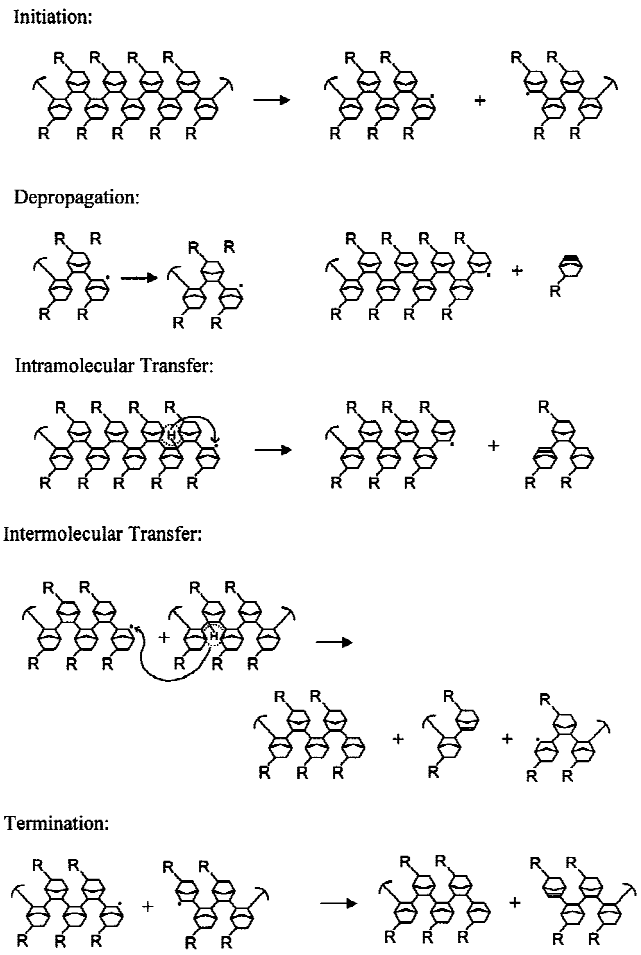

FIG. 11. Decomposition mechanism for ionized norbornane.

Proposed Structure	Methyl	Butyl	Butyl/TES	Hexyl
	**C_8H_{12}**	**$C_{11}H_{18}$**	**$C_{11}H_{18}$**	**$C_{13}H_{21}$**
	C_8H_{11}, C_8H_{13}	$C_{11}H_{17}$, $C_{11}H_{18}$	$C_{11}H_{17}$, $C_{11}H_{18}$	$C_{13}H_{21}$
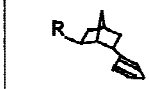	**$C_{13}H_{17}$**	**$C_{16}H_{23}$**	**$C_{16}H_{23}$**	**$C_{18}H_{27}$**
	$C_{13}H_{17}$	$C_{16}H_{23}$, $C_{16}H_{24}$	$C_{16}H_{23}$, $C_{16}H_{24}$	$C_{18}H_{27}$
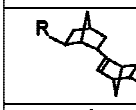	**$C_{16}H_{23}$**	**$C_{22}H_{35}$**	**$C_{22}H_{35}$**	**$C_{26}H_{43}$**
	$C_{16}H_{23}$	$C_{22}H_{36}$	$C_{22}H_{35}$, $C_{22}H_{36}$	$C_{26}H_{44}$
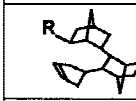	**$C_{21}H_{31}$**	**$C_{27}H_{43}$**	**$C_{27}H_{43}$**	**$C_{31}H_{51}$**
	$C_{21}H_{30}$	$C_{27}H_{43}$, $C_{27}H_{44}$	$C_{27}H_{42}$, $C_{27}H_{43}$	$C_{31}H_{51}$
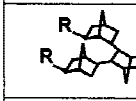	**$C_{24}H_{37}$**	**$C_{33}H_{55}$**	**$C_{33}H_{55}$**	**$C_{39}H_{67}$**
	$C_{24}H_{34}$, $C_{24}H_{36}$	$C_{33}H_{56}$	$C_{33}H_{55}$, $C_{33}H_{56}$	$C_{39}H_{67}$
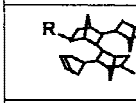	**$C_{29}H_{41}$**	**$C_{38}H_{61}$**	**$C_{38}H_{61}$**	**$C_{44}H_{73}$**
	$C_{29}H_{42}$	$C_{38}H_{61}$	$C_{38}H_{61}$	$C_{44}H_{73}$
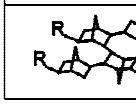		**$C_{44}H_{74}$**		
		$C_{44}H_{73}$		

FIG. 12. Peak identifications for MePNB, BuPNB, and HxPNB.

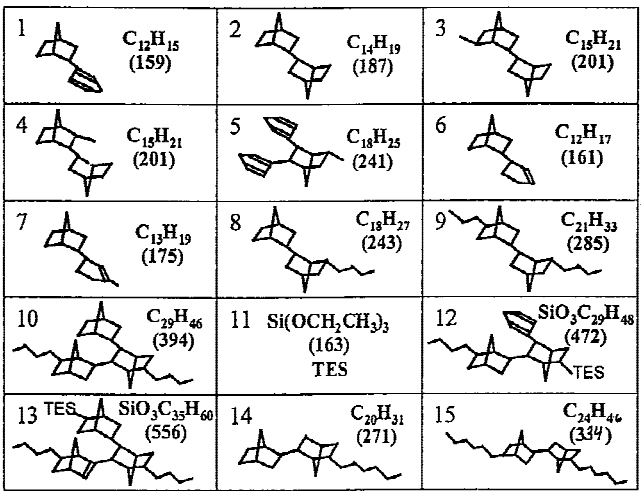

FIG. 13. High molecular weight peak identification for MePNB, BuPNB, BuTESPNB, and HxPNB.

peaks moved in tandem throughout the degradation process. Increasing temperature tended to produce a proportional increase in the production rate of all species. A comparison of the dynamic mass spectrometry samples at 5 and 10 °C/min corresponded well with the increases in weight loss rate from the dynamic TGA. The only component of the spectra that showed considerable deviation from the behavior was peak 66, the major decomposition product of norbornene. If depropagation reactions dominated the degradation process, one would expect to see prominent peaks for the monomer. In the case of polynorbornene, this would correspond to the ionization decomposition products of a functionalized norbornene. If this molecule behaves like norbornene, the retro-Diels–Alder reaction would be strongly favored, and a prominent peak at 66 would be expected. In all samples, the initial major peak was 66. With increasing conversion, the high molecular weight oligomer products and their decomposition descendents increased in proportion. The peak for 66 consistently dropped from a high intensity peak to one stabilizing to the other degradation products. The bulk degradation mechanism is influenced by the ratio of depropagation to transfer, which is dependent on the free radical produced in the initiation step and on the availability of reactive atoms (hydrogen) in the polymer system.[22] Note, in the depropagation reaction, a radical-terminated polymer chain loses an unsaturated monomer unit (no hydrogen transfer needed) while the transfer reaction requires a hydrogen atom to be transferred, resulting in saturated products. Based on the mass spectra for these polymers, it appears that initially the depropagation reaction is favored, but with increasing conversion the transfer reactions become more dominant. One explanation for the shift from depropagation to transfer reactions may be the increasing segmental mobility of the polymer chain with increasing fragmentation of the polymer backbone. With increased freedom of movement, the radical polymer ends could abstract hydrogen by attacking adjacent molecules.

IV. CONCLUSIONS

Four functionalized polynorbornenes (MePNB, BuPNB, HxPNB, and a 10% TESPNB, 90% BuPNB copolymer) were studied by dynamic and isothermal TGA, and mass spectrometry. In all four cases, the PNB degradation could be described by first-order reaction and an activation energy in the range of 229.6 ± 12.5. The side groups tended to have a small effect on the thermal stability of the molecule with slightly higher thermal stability with increasing alkyl chain length and the presence of electron-withdrawing groups (triethoxysilane). The degradation mechanism results from the scission of the linkages joining the bicyclic repeat units. Based on the first-order reaction kinetics, these reactions are believed to occur in a chain-wise manner. Initially this is achieved by depropagation reactions, but with increasing conversion, intra- and intermolecular transfer reactions dominate.

ACKNOWLEDGMENTS

The support of BF Goodrich, and intellectual contributions of Robert Shick and S.A. Allen are gratefully acknowledged.

REFERENCES

1. A.W. Anderson and M.G. Merckling, U.S. Patent No. 2 721 189 (1955).
2. L.E. McKeon and P.S. Starcher, U.S. Patent No. 3 330 815 (1967).
3. W. Kaminsky, Makromol. Chem. Macromol. Symp. **47,** 83 (1991).
4. W. Kaminsky, J. Mol. Cat. **74,** 109 (1992).
5. B. Goodall, G. Benedickt, L. McIntosh III, and D. Barnes, U.S. Patent No. 5 468 819 (1995).
6. B. Goodall, G. Benedickt, L. McIntosh III, and D. Barnes, U.S. Patent No. 5 569 730 (1996).
7. B. Goodall, G. Benedickt, L. McIntosh III, and D. Barnes, U.S. Patent No. 5 571 881 (1996).
8. B. Goodall, L. McIntosh III, and D. Barnes, U.S. Patent No. 5 677 405 (1997).
9. B. Goodall, W. Risse, and J. Mathew, U.S. Patent No. 5 705 503 (1998).
10. B. Goodall, G. Benedickt, L. McIntosh III, D. Barnes, and L. Rhodes, U.S. Patent No. 5 741 869 (1998).
11. L. McIntosh, B. Goodall, R. Shick, and S. Jayaraman, U.S. Patent No. 5 912 313 (1999).
12. K. Makovetsky, E. Frinkelstein, V. Bykov, A. Bagdasayan, B. Goodall, and L. Rhodes, U.S. Patent No. 5 929 181 (1999).
13. L. McIntosh, B. Goodall, R. Shick, and S. Jayaraman, U.S. Patent No. 6 031 058 (2000).
14. N.R. Grove, P.A. Kohl, S.A. Allen, S. Jayaraman, and R. Shick, J. Polymer Sci **37,** 3003 (1999).
15. D. Appell, *Optical Polymers Heat and Greet,* OE Reports, No. 197 May (2000).
16. K. Patterson, M. Somervell, and W.C. Grant, Solid State Technol., **43,** 41 (2000).
17. K.D. Dorkenoo, P.H. Pfromm, and M.E. Rezac, J. Polymer Sci. **36,** 797 (1998).
18. P.A. Kohl, Q. Zhao, K.S. Patel, D.S. Schmidt, S.A. Bidstrup, R. Shick, and S. Jayraman, Electrochem. Solid State Lett. **1,** 49 (1998); P.A. Kohl, D.M. Bhusari, M. Wedlake, C. Case, B.C. Lee, R.J. Gutmann, and R. Shick, Electron Dev. Lett. **21,** 557 (2000).
19. T. Ozawa, Bull. Chem. Soc. Jpn. **38,** 1881 (1965).
20. L. Reich et al. *Macromolecular Reviews* (Wiley Interscience, New York, 1966), Vol. 1, p. 173ff.
21. *An Introduction to Spectroscopic Methods for the Identification of Organic Compounds,* edited by F. Scheinmann (Pergamon Press, Oxford, United Kingdom, 1973), Vol. 2.
22. *Addition Polymers: Formation and Characterization,* edited by D.A. Smith (Plenum Press, New York, 1968).
23. R.P. Lattimer, J. Anal. Appl. Pyrolysis **139,** 115 (1997).